Published in final edited form as:
J Am Chem Soc. 2012 January 25; 134(3): 1501–1503. doi:10.1021/ja2112788.

Dynamics and mechanism of DNA repair in a biomimetic system: Flavin-thymine dimer adduct

Ya-Ting Kao, **Qin-Hua Song**, **Chaitanya Saxena**, **Lijuan Wang**, and **Dongping Zhong***
Department of Physics and Department of Chemistry and Biochemistry, Programs of Biophysics, Chemical Physics and Biochemistry, 191 West Woodruff Avenue, The Ohio State University, Columbus, OH

Abstract

To mimic photolyase for efficient repair of UV-damaged DNA, numerous biomimetic systems have been synthesized but all show low repair efficiency. The molecular mechanism of this low efficient process is still poorly understood. Here, we reported our direct mapping of the repair processes of a flavin-thymine dimer adduct with femtosecond resolution. We followed the entire dynamic evolution and observed direct electron transfer from the excited flavin to the thymine dimer in 79 picoseconds (ps). We further observed two competitive pathways, productive dimer ring splitting within 435 ps and futile back electron transfer in 95 ps. Our observation reveals that the underlying mechanism for the low repair quantum yield of flavin-thymine dimer adducts is the short-lived excited flavin moiety and the fast dynamics of futile back electron transfer without repair.

One of the detrimental effects of UV radiation on the biosphere is the formation of cyclobutane pyrimidine dimers (CPDs) which causes DNA damage and can lead to skin cancer. Photolyase is a photoenzyme and responsible for repairing UV-damaged DNA in many organisms.[1] In our recent studies on *E. coli* CPD photolyase,[2,3] we captured the radical intermediates and revealed the electron-transfer (ET) mechanism in DNA repair. Upon excitation with blue light, CPD photolyase, a flavin-containing enzyme, transfers an electron from the isoalloxazine ring of cofactor $FADH^-$ to the dimer and then the cyclobutane ring splits spontaneously, following by electron return to restore the active form of cofactor $FADH^-$. The DNA repair by photolyase is very efficient with the quantum yield of more than 0.80–0.95.[1,3] However, numerous biomimetic systems have been synthesized to mimic the repair function but all have shown low repair efficiency, for example, 0.016–0.062 for flavin-thymine dimer systems[4,5] and 0.06–0.40 for indole-thymine dimer systems.[6,7] The molecular mechanism of these low efficient processes have not been understood.[8,9] Here, we report our direct mapping of repair processes in a biomimetic flavin-thymine dimer adduct by following the temporal evolution of reactants and intermediates using femtosecond (fs) spectroscopy. By capturing the complete repair photocycle and comparing to that of CPD photolyase, we can understand how CPD photolyase achieves its high repair efficiency.

Instead of simply using a mixture solution of thymine dimer and flavin, a covalent linkage between the lumiflavin (LF) and thymine dimer (T<>T) is designed to hold flavin photosensitizer and dimer together (Figure 1). The oxidized flavin-thymine dimer adduct

Corresponding Author zhong.28@asc.ohio-state.edu.

ASSOCIATE CONTENT

Supporting Information. A summary of the kinetic fitting model. This material is available free of charge via the Internet at http://pubs.acs.org.

(LF-T<>T) was synthesized, purified and characterized as described previously.[5] The fully-reduced flavin-thymine dimer (LFH^{-}-T<>T) and the fully-reduced flavin ($FMNH^{-}$) were generated from 350-μM oxidized samples through chemical reduction[10] with 250 mM sodium borohydride in 12.5 mM phosphate buffers at pH 8.5 under anaerobic conditions. Complete reduction was confirmed by both the UV/visible absorption and, more importantly, the fluorescence spectrum as judged by a single emission peak, indicating a single species without a mixture of different redox flavins. The molecular structures of LFH^{-}-T<>T and LFH^{-} highlighted with pink and blue background are shown in Figure 1, respectively. The absorption and emission spectra of fully-reduced $FMNH^{-}$ in solution are shown in inset of Figure 1. The absorption spectrum is consistent with previous studies,[4,11] and the emission spectrum is similar to our earlier report of $FADH^{-*}$ emission.[12] Upon 360-nm excitation, we observed weak fluorescence emission peaked at 435 nm for fully-reduced $FMNH^{-}$. More importantly, we observed the excitation-wavelength dependence of emission spectra.[12] Also, the fluorescence intensity of fully-reduced flavin in solution is much weaker than that observed in photolyase,[12] suggesting very different dynamic behaviors of fully-reduced flavin in two environments (see below).

We first characterized the excited $FMNH^{-*}$ dynamics using fs-resolved fluorescence spectroscopy. By monitoring the weak $FMNH^{-*}$ emission at 450 nm, the fluorescence transient in the absence of dimer exhibits multiple decay dynamics in 5.8 ps (82%), 35 ps (16%) and 1.5 ns (2%) as shown in Figure 1. Such multiple-decay dynamics reflect the ultrafast deactivation of the excited $FMNH^{-*}$.[12] In contrast to the excited $FMNH^{-*}$ in solution, our previous studies[2] showed the dynamics of the excited $FADH^{-*}$ in photolyase with a dominant long lifetime of 1.3 ns, and suggested that the butterfly bending of the isoalloxazine ring be a critical motion and directly control the excited-state dynamics of fully-reduced flavins.[12] In solution, free LFH^{-} easily changes its conformation and in the proteins it is highly restricted, geometrically and electrostatically. Thus, the more flexible the environment, the shorter the excited state lifetime of fully-reduced flavin.

In the presence of the thymine dimer, the fluorescence transient exhibits faster dynamics, indicating the presence of another reaction channel, the ET reaction. The potential for flavin ($FMNH^{\bullet}/FMNH^{-}$) is −0.172 V vs. NHE[13] and for thymine dimer ($T<>T/T<>T^{-}$) is −1.96 V vs. NHE.[14] Using 500-nm absorption tail as the 0-0 transition energy of 2.48 eV, we obtained a net ΔG^{0} of −0.692 eV. Thus, the intramolecular ET between the excited flavin and thymine dimer is energetically favorable. By considering the ET reaction in each deactivation process of excited LFH^{-*} (Figure 1), we obtained an ET dynamics in 79 ps (τ_{ET}) and thus the quantum yields, $\tau_{ET}^{-1}/(\tau_{ET}^{-1}+\tau_{d}^{-1})$, of ET are 0.068, 0.307 and 0.950 in the three deactivation processes, resulting in the first-step ET quantum yield (φ_{ET}) of 0.124. In photolyase, even though the average ET dynamics of 250 ps is slower than 79 ps, the long-lived excited flavin ($FADH^{-*}$) of 1.3 ns results in a much higher ET quantum yield of ~0.85.[2,3,15,16] This observation reveals that the ultrafast deactivation of the excited fully-reduced flavin in all biomimetic flavin-thymine dimer adducts already leads to a low quantum yield in the first-step forward electron transfer.

According to recent quantum chemical calculations,[8,9,17,18] the splitting of the C5-C5′ bond of the anionic dimer ($T<>T^{-}$) is a downhill reaction and occurs in less than 1 ps (τ_{SP1}), as indicated in Figure 2A. The C5-C5′ bond splitting in photolyase was determined to be less than 10 ps.[3,16] This step is too fast to be observed here because the intermediate could not be accumulated due to the slow formation time (79 ps). After the C5-C5′ ultrafast splitting, the reaction can evolve along two pathways, the nonproductive pathway including back ET (τ_{BET}) and ring reclosure without repair or the repair channel including the C6-C6′ bond splitting (τ_{SP2}) and then electron return (τ_{ER}) after repair. Based on our recent studies on the thymine dimer repair by photolyase using UV/visible detection, the C6-C6′ splitting is

decoupled from the electron return.[3] For clarity, here, we described $LFH^{\bullet}$ formed after the C5-C5′ bond splitting as the initially formed $LFH^{\bullet}$ (with cyan underline in Figure 2A) and $LFH^{\bullet}$ after the C6-C6′ bond splitting as the branched $LFH^{\bullet}$ (with purple underline in Figure 2A).

By knowing the forward ET dynamics of LFH^{-*}-T<>T, we can map out the temporal evolution of $LFH^{\bullet}$ by probing at wavelengths from 580 to 710 nm to follow the CPD repair. For example, we observed the similar transients probed at 580 and 625 nm, but drastically different from that probed at 710 nm (Fig. 2B), due to the capture of the radical $LFH^{\bullet}$ (blue curve in Fig. 2B). At 580 nm probing, we observed three different dynamic components of $LFH^{\bullet}$ (the kinetic fitting model in the Supporting Information). The dominant one is from the initially formed $LFH^{\bullet}$ with a decay dynamics of 78 ps ($(\tau_{SP2}^{-1}+\tau_{BET}^{-1})^{-1}$ in Figure 2A and dashed cyan curve in Figure 2B). In our recent studies of indole-thymine dimer adduct through transient absorption in UV range, we observed dimer splitting in 450 ps (τ_{SP2}) in aqueous solution. Here, at 580 nm probing, we obtained dimer splitting in 435 ps (τ_{SP2}) and back electron transfer in 95 ps (τ_{BET}). Two minor $LFH^{\bullet}$ components are from the branched $LFH^{\bullet}$ (dashed purple and lime green curves in Figure 2B). For one minor component with more than 85% of the total branched $LFH^{\bullet}$ signal, we observed a formation mainly in 23± 12 ps (τ_{ER}) and a complex decay (dashed purple curve in inset of 2B) mainly in around ~80 ps. The 23 ps actually is for the electron return process. The slower formation and faster decay result in apparent reverse kinetics and less $LFH^{\bullet}$ accumulation. The ER of 23 ps is the electron return from linked thymine T_1 (Figure 1 inset) to $LFH^{\bullet}$ to restore active form LFH^{-}. The other minor component of less than 15% exhibits a long plateau (dashed lime green curve in inset of Fig. 2B), indicating that the negative charge could stay in the distant thymine T_2, leading to a long-lived $LFH^{\bullet}$. At 710-nm probing, we observed the dominant LFH^{-*} and a minor $LFH^{\bullet}$ signal with the similar dynamics probed at 580 and 620 nm.

Knowing the potential for thymine base (T/T^{-}) of −1.90 V vs. NHE,[14] we obtained a net ΔG^0 of −1.728 eV for electron return. Consider the net ΔG^0 values and the rates of both ET and ER, we estimate that the distance between flavin and thymine dimer is about 7Å and the reorganization energy is about 1.5 eV.[16] Hence, the ET reaction lies in the Marcus normal region and the ER reaction lies in the inverted region. Also, the faster dynamics of ER compared with ET is due to a low activation energy and might also be facilitated through hot vibration modes of products.[19–21] For BET, because it occurs along the splitting coordinate and its free energy is greatly reduced during the splitting, the absolute value of the net ΔG^0 should be much smaller than 1.788 eV (−1.96 eV+0.172 eV= −1.788 eV).[8,9] Thus, BET probably lies in the normal region with a small driving force,[8,16] resulting in the dynamics of 95 ps which is slower than those of ET and ER.

The fast BET of 95 ps in solution indicates a relatively unstable charge-separated intermediate ($LFH^{\bullet}$-T<>T^{-}), leading to a significant competition between ring splitting (435 ps) and futile back electron transfer. The efficiency of the dimer ring splitting with electron return is 0.179 ($\varphi_{SP} = \tau_{BET}/(\tau_{SP2}+\tau_{BET})$). Considering the ET quantum yield of 0.124 (φ_{ET}) acquired by the fluorescence experiment, we obtained the total repair efficiencies of 0.022 ($\Phi_{total}=\varphi_{ET}\times\varphi_{SP}$) which is about one-third of the reported value (0.062) by steady-state measurements, but on the same order.[4] Our observation reveals that the underlying molecular mechanism for the low repair quantum yield of all flavin-thymine dimer adducts is the short-lived excited flavin and the fast dynamics of futile back electron transfer. In contrast, in CPD photolyase, the enzyme can utilize geometric restriction and electrostatic interactions to confine the flavin cofactor and lengthen its excited-state lifetime. This long-lived cofactor could exist long enough to react with CPDs to form a charge-separated intermediate and thus reach a high ET quantum yield. Moreover, the active site stabilizes charge-separated intermediate in photolyase (>1 ns) and speeds up the ring splitting within

90 ps.[3] Such modulation of the dynamics leaves enough time to cleave the ring, resulting in a high splitting efficiency. These two high efficient processes lead to a perfect repair of damage DNA by photolyase.

Supplementary Material

Refer to Web version on PubMed Central for supplementary material.

Acknowledgments

This work was supported in part by the NIH grant GM074813 and the Packard Foundation fellowship to DZ. Thank Dr. Xunmin Guo for helpful discussion.

References

1. Sancar A. Chem. Rev. 2003; 103:2203–2237. [PubMed: 12797829]
2. Kao Y-T, Saxena C, Wang L, Sancar A, Zhong D. Proc. Natl. Acad. Sci. U.S.A. 2005; 102:16128–16132. [PubMed: 16169906]
3. Liu Z, Tan C, Guo X, Kao Y-T, Li J, Wang L, Sancar A, Zhong D. Proc. Natl. Acad. Sci. U.S.A. 2011; 108:14831–14836. [PubMed: 21804035]
4. Epple R, Wallenborn E-U, Carell T. J. Am. Chem. Soc. 1997; 119:7440–7451.
5. Song Q-H, Tang W-J, Ji X-B, Wang H-B, Guo Q-X. Chem. Eur. J. 2007; 13:7762–7770. [PubMed: 17568458]
6. Song Q-H, Tang W-J, Hei X-M, Wang H-B, Guo Q-X, Yu S-Q. Eur. J. Org. Chem. 2005; 1097
7. Kim S-T, Hartman RF, Rose SD. Photochem. Photobiol. 1990; 52:789–794. [PubMed: 2089427]
8. Hassanali AA, Zhong D, Singer SJ. J. Phys. Chem. B. 2011; 115:3848–3859. [PubMed: 21417374]
9. Hassanali AA, Zhong D, Singer SJ. J. Phys. Chem. B. 2011; 115:3860–3871. [PubMed: 21417372]
10. Müller F, Massey V, Heizmann C, Hemmerich P, Lhoste J-M, Gould DC. Eur. J. Biochem. 1969; 9:392–401. [PubMed: 4307593]
11. Ghisla S, Massey V, Lhoste J-M, Mayhew SG. Biochemistry. 1974; 13:589–597. [PubMed: 4149231]
12. Kao Y-T, Saxena C, He T-F, Guo L, Wang L, Sancar A, Zhong D. J. Am. Chem. Soc. 2008; 130:13132–13139. [PubMed: 18767842]
13. Draper RD, Ingraham LL. Arch. Biochem. Biophys. 1968; 125:802–808. [PubMed: 5671043]
14. Scannell MP, Fenick DJ, Yeh S-R, Falvey DE. J. Am. Chem. Soc. 1997; 119:1971–1977.
15. Kao Y-T, Saxena C, Wang L, Sancar A, Zhong D. Cell Biochem. Biophys. 2007; 48:32–44. [PubMed: 17703066]
16. Liu Z, Guo X, Tan C, Li J, Kao Y-T, Wang L, Sancar A, Zhong D. J. Am. Chem. Soc. in review.
17. Masson F, Laino T, Tavernelli I, Rothlisberger U, Hutter J. J. Am. Chem. Soc. 2008; 130:3443–3450. [PubMed: 18284237]
18. Saettel NJ, Wiest O. J. Am. Chem. Soc. 2001; 123:2693–2694. [PubMed: 11456951]
19. Jortner J, Bixon M. J. Chem. Phys. 1988; 88:167–170.
20. Nagasawa Y, Yartsev AP, Tominaga K, Bisht PB, Johnson AE, Yoshihara K. J. Phys. Chem. 1995; 99:653–662.
21. Barbara PF, Meyer TJ, Ratner MA. J. Phys. Chem. 1996; 100:13148–13168.
22. Gladkikh V, Burshtein AI, Feskov SV, Ivanov AI, Vauthey E. J. Chem. Phys. 2005; 123:244510. [PubMed: 16396552]

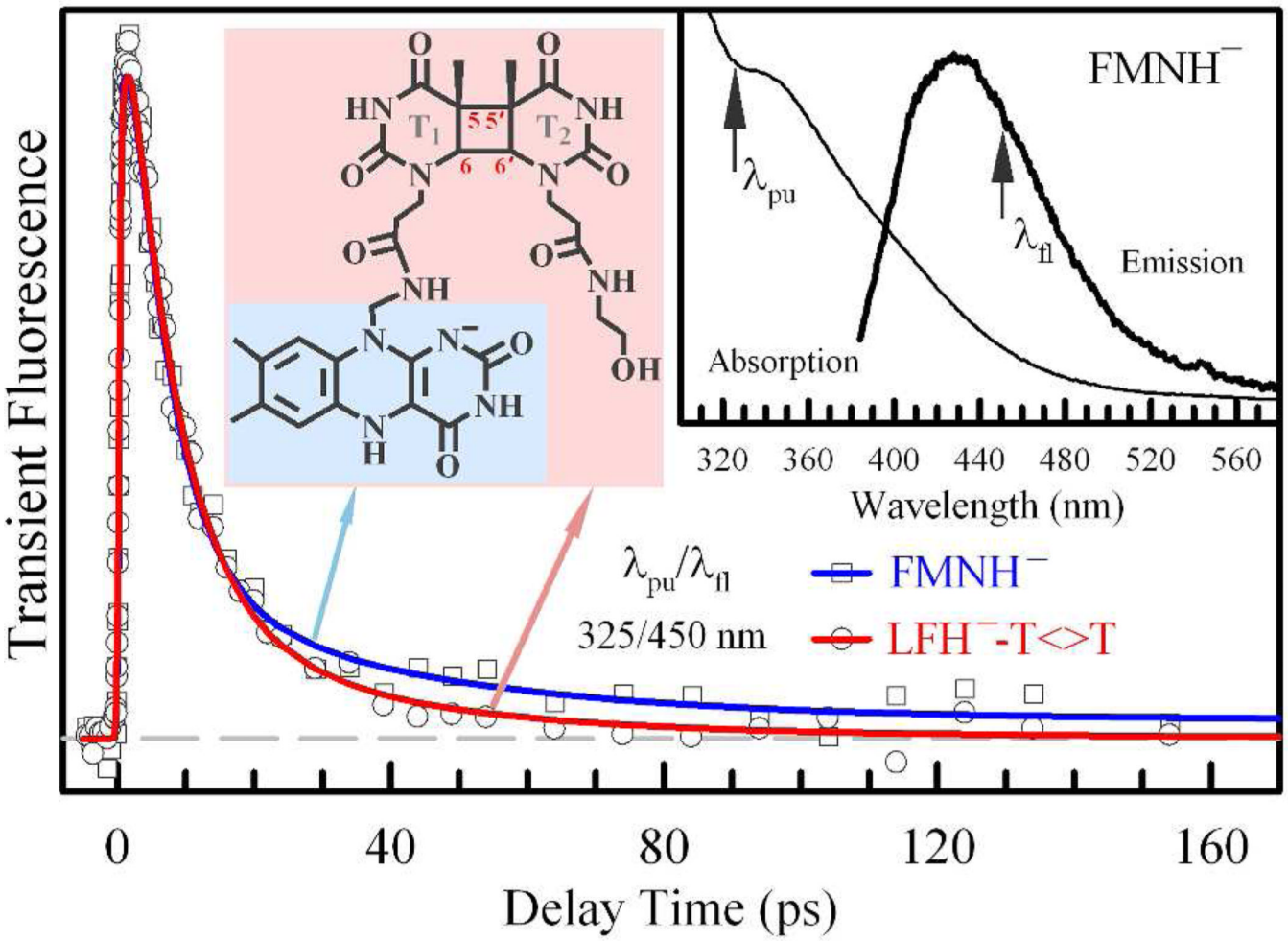

Figure 1.

The femtosecond-resolved fluorescence transients of reduced $FMNH^-$ and LFH^--T<>T gated at 450 nm, upon 325-nm excitation. The molecular structures of LFH^--T<>T and LFH^- are highlighted with pink and blue background, respectively. *Inset* shows absorption and emission spectra (360 nm excitation) of reduced $FMNH^-$. Two arrows indicate the pump wavelength and gated fluorescence emission.

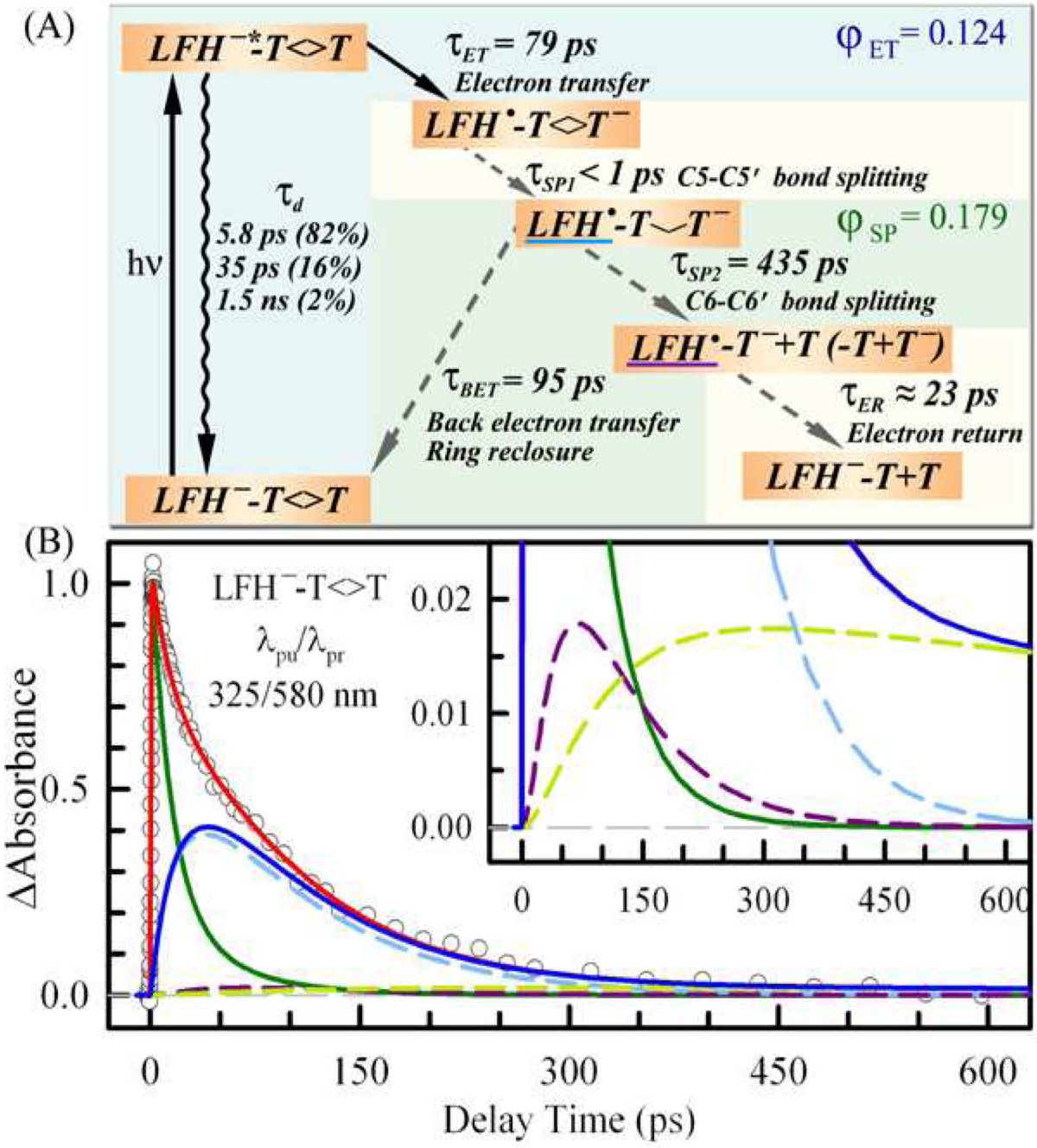

Figure 2.

(A) The repair scheme with forward electron transfer (τ_{ET}) after light excitation, ultrafast first C5-C5′ bond splitting (τ_{SP1}), back electron transfer (τ_{BET}) and ring reclosure without repair, and the repair channel including C6-C6′ bond splitting (τ_{SP2}) and electron return (τ_{ER}). (B) The fs-resolved absorption signal of LFH^{-*}-T<>T probed at 580 nm, upon 325-nm excitation, with both LFH^{-*}-T<>T (green curve and mainly probed at 710 nm) and $LFH^{\bullet}$ detection (blue curve). The total $LFH^{\bullet}$ signal is from the one dominant contribution of the initially formed $LFH^{\bullet}$ (dashed cyan curve) and two minor contributions of the branched $LFH^{\bullet}$ in the repair channel (≥85%, dashed purple; <15%, dashed lime green). Note that a

minor plateau from the deactivation channels in the 710-nm transient was removed for clarity. *Inset* shows the dynamics of two fitted minor channels.